De Novo Pathogenic *SCN8A* Mutation Identified by Whole-Genome Sequencing of a Family Quartet Affected by Infantile Epileptic Encephalopathy and SUDEP

Krishna R. Veeramah,[1] Janelle E. O'Brien,[4] Miriam H. Meisler,[4] Xiaoyang Cheng,[5] Sulayman D. Dib-Hajj,[5] Stephen G. Waxman,[5] Dinesh Talwar,[6,7,9] Santhosh Girirajan,[10] Evan E. Eichler,[10] Linda L. Restifo,[2,7,8] Robert P. Erickson,[3,6] and Michael F. Hammer[1,*]

Individuals with severe, sporadic disorders of infantile onset represent an important class of disease for which discovery of the underlying genetic architecture is not amenable to traditional genetic analysis. Full-genome sequencing of affected individuals and their parents provides a powerful alternative strategy for gene discovery. We performed whole-genome sequencing (WGS) on a family quartet containing an affected proband and her unaffected parents and sibling. The 15-year-old female proband had a severe epileptic encephalopathy consisting of early-onset seizures, features of autism, intellectual disability, ataxia, and sudden unexplained death in epilepsy. We discovered a de novo heterozygous missense mutation (c.5302A>G [p.Asn1768Asp]) in the voltage-gated sodium-channel gene *SCN8A* in the proband. This mutation alters an evolutionarily conserved residue in Nav1.6, one of the most abundant sodium channels in the brain. Analysis of the biophysical properties of the mutant channel demonstrated a dramatic increase in persistent sodium current, incomplete channel inactivation, and a depolarizing shift in the voltage dependence of steady-state fast inactivation. Current-clamp analysis in hippocampal neurons transfected with p.Asn1768Asp channels revealed increased spontaneous firing, paroxysmal-depolarizing-shift-like complexes, and an increased firing frequency, consistent with a dominant gain-of-function phenotype in the heterozygous proband. This work identifies *SCN8A* as the fifth sodium-channel gene to be mutated in epilepsy and demonstrates the value of WGS for the identification of pathogenic mutations causing severe, sporadic neurological disorders.

Massively-parallel-sequencing technologies are revolutionizing the process of discovering genetic variants that cause disease.[1] Neurodevelopmental disorders such as epilepsy, autism spectrum disorders (ASDs), intellectual disability (ID), and schizophrenia represent a considerable challenge for molecular genetic analysis because of marked genetic heterogeneity, environmental effects on the severity of symptoms, and the frequent co-occurrence of seizures, autism, and cognitive phenotypes. Studies of copy-number variation (CNV) have demonstrated the contribution of de novo variants in these disorders.[2,3] However, CNVs only appear to contribute to between 10% and 25% of affected cases.[4] It is hypothesized that rare or novel point mutations might contribute to many of the remaining cases under the CD/MRV (common disease/multiple rare variant) model.[5] When the observed phenotype is particularly severe and there is no prior family history of the disorder, it is reasonable to consider a disease model that involves a dominant de novo mutation. Support for this model comes from studies of epileptic encephalopathies, in which de novo mutations of the sodium-channel gene *SCN1A* (MIM 182389) are a major cause of Dravet Syndrome (MIM 607208),[6] whereas de novo mutations in *STXBP1* (MIM 602926) and *ARX* (MIM 300382) have been found in a number of individuals with early infantile epileptic encephalopathy (MIM 308350).[7] When such mutations arise, they are expected to be quickly removed by strong purifying selection (because affected individuals rarely reproduce) and hence would be extremely rare or unique in the population. Although the human mutation rate is on the order of 1×10^{-8} to 2×10^{-8} per site per generation,[8,9] thousands of genes are potentially involved in neurodevelopment,[10] suggesting that the number of de novo pathogenic mutations could be substantial. Thus, although each individual is expected to have only ~1 de novo mutation per exome,[11] a model of rare mutations across many genes might explain why severe neurological disorders are relatively common.[12]

Whole-exome sequencing of parent-offspring trios offers a cost-effective method for screening coding regions for mutations and has been successful in identifying candidate de novo variants in sporadic cases of ID,[12] ASDs,[13] and schizophrenia.[14] However, the limitations of current exome capture and sequencing methodologies include incomplete or variable coverage of exons and the inability to infer ploidy across the genome or survey regulatory variation. Whole-genome sequencing (WGS) studies are not limited by these aspects, and when they are implemented in a quartet framework, they have many attractive analytical advantages. For example, it is possible to precisely infer haplotype phase and the location of recombination

[1]Arizona Research Laboratories Division of Biotechnology, [2]Department of Neuroscience, [3]Department of Molecular and Cellular Biology, University of Arizona, Tucson, AZ, 85721, USA; [4]Department of Human Genetics, University of Michigan, Ann Arbor, MI 48109-5618, USA; [5]Department of Neurology, Yale School of Medicine, New Haven, CT 06520-8018, USA; [6]Department of Pediatrics, [7]Department of Neurology, [8]Department of Cellular and Molecular Medicine, Arizona Health Science Center, Tucson, AZ 85724, USA; [9]Center for Neurosciences, Tucson, AZ 85718, USA; [10]Department of Genome Sciences, Howard Hughes Medical Institute, University of Washington, Seattle, WA 98195, USA
*Correspondence: mfh@email.arizona.edu
DOI 10.1016/j.ajhg.2012.01.006.

events,[9,15] which can substantially improve the detection and correction of sequencing errors.

In this study, we apply WGS to a family quartet affected by a sporadic case of severe epileptic encephalopathy. Informed consent was obtained from the family quartet, and the study was approved by the University of Arizona institutional review board. The female proband presented at 6 months of age with unexplained refractory epilepsy consisting of early-onset brief (2–10 s) generalized seizures. When she was 4 years old, the seizure phenotype changed to epileptic spasms. In addition to early- and later-onset epilepsy, she manifested intellectual disability, developmental delay, hypotonia, and difficulties with coordination and balance. The proband was able to walk independently just before she turned 3 years old and started to use 5- to 6-word phrases before the age of 4. With the onset of epileptic spasms, her speech and language skills began to regress over the course of 1–2 years, causing her to occasionally use single words only. These language and communication problems, in combination with regression in social interaction and the development of obsessive-compulsive and repetitive behaviors, led to the classification of autism when she was 5 years old.

When the proband was 6 months old, initial electroencephalograms (EEGs) showed bifrontal spikes and brief bursts of frontocentrally predominant generalized spike-wave activity lasting for a few seconds at a time. Some of the bursts were associated with clinical seizures. Initial seizures showed no association with fever or illness and occurred very frequently up to 40–50 times per day. Subsequent EEGs after the proband turned 5 years old showed diffuse slowing, multifocal spikes, bifrontal and frontally predominant generalized spikes, and runs of frontally predominant slow spike-wave discharges. Several brain magnetic resonance imaging (MRI) scans performed when she was between 6 months and 15 years of age were normal, and a PET scan failed to show any focal abnormalities. At 15 years of age, the proband died from sudden unexplained death in epilepsy (SUDEP). An autopsy showed pulmonary edema and only mild temporal-lobe subpial gliosis.

The proband was the first-born female child of two phenotypically unaffected parents. Her male sibling showed neither evidence of epilepsy nor any major cognitive or motor deficits. Given the severity of the disorder and a negative family history, we hypothesized the involvement of a de novo mutation. To detect rare CNVs, we performed array-based comparative genomic hybridization (CGH) experiments. We utilized a custom 2x400K Agilent microarray targeted to genomic hotspot regions flanked by segmental duplications or Alu repeats, and we used median probe spacing of 500 bp and probe spacing of 14 kb in the genomic backbone. After quality-control filtering and manual curation, we identified 93 CNV calls (Table S1, available online). To identify rare variants of pathogenic significance, we compared the CNV pattern to the global CNV map developed from 8,329 controls[16] and 377 additional controls analyzed on the same microarray platform. Allowing for a frequency of <1% in the general population in regions with sufficient coverage (>10 probes), we did not find any novel pathogenic CNVs in our proband or any that were previously associated with known genomic disorders.[4]

We therefore carried out WGS to look for candidate point mutations or small insertions or deletions. WGS was performed for the quartet by Complete Genomics (CG). CG performs a massively parallel short-read sequence-by-ligation methodology.[17] Details of library generation, read-mapping to the NCBI reference genome (Build 37, RefSeq Accession numbers CM000663–CM000686), local de novo assembly, and variant-calling protocols have been previously described.[9,17] Mean unique sequence coverage ranged from 57× to 77×, and 96%–97% of the genome was considered fully called across the quartet. A nucleotide position is determined to be fully called if it meets a minimum required confidence-score threshold (20 dB for homozygotes and 40 dB for heterozygotes), which is calculated by taking into account read depth, base-call quality values, and mapping probabilities. All variants were annotated with ANNOVAR[18] on the basis of the UCSC Known Genes Hg19 database, which covers 84,177,555 bp of coding sequence. From the reference sequence, we identified 31,931 variants within exons or at splice-site boundaries on all chromosomes. There were 13,395 potentially function-altering variants on autosomes within the quartet.

To increase variant call quality by using Mendelian inheritance rules and information inherent in the quartet, we applied a hidden Markov model (HMM)[9] to infer the position of recombination events that demarcate inheritance state (IS) blocks between the two siblings; this model has been shown to identify ~70% of expected CG-generated sequencing errors. Among the potentially functional variants, we were able to identify 205 errors on the basis of IS consistency analysis, and we were able to unambiguously recover the complete quartet genotype of 58% (1,229/2,103) of the variants that contained missing data.

For the 11,292 variants fully called within the quartet, 34 violated the Mendelian inheritance rules and would be consistent with a de novo mutation within the proband (i.e., the mutation is present in the proband but not in either parent or the sibling). Ten of these variants were discarded because they were found in the 1,000 Genome Project May 2011 release or the 69 CG public genomes, or they were mapped within (1) error-prone regions (defined as containing at least 5 Mendelian inheritance errors and no more than 1,000 bp separating any two errors), (2) known segmental duplications (Database of Genomic Variants), (3) a repeat sequence (UCSC-defined tracks), (4) suspicious genomic blocks identified by the HMM IS block analysis, or (5) sites that differed significantly in coverage from the genome-wide average. Sanger sequencing demonstrated that 23 of the remaining 24 candidates were false positives, leaving a single, true de novo variant in the proband.

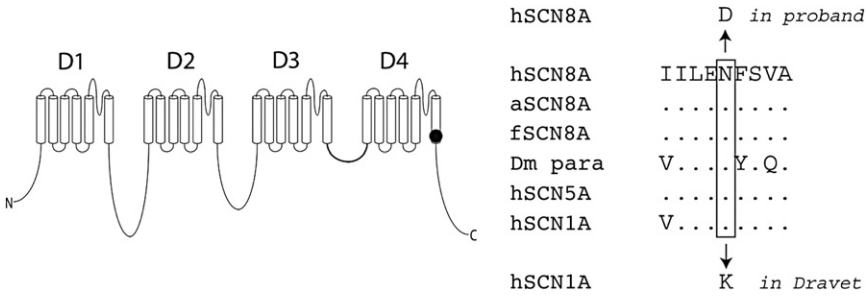

Figure 1. The De Novo Proband Substitution p.Asn1768Asp in Sodium-Channel SCN8A

The altered amino acid residue is located at the cytoplasmic end of transmembrane segment 6 in domain 4 of the channel (for simplicity of display, we use 1-letter amino acid codes). Residue 1768 is evolutionarily conserved in mammalian and invertebrate sodium channels, as indicated by the examples shown on the right. The polar asparagine residue is altered to the charged residue aspartate in our proband. A substitution in the corresponding residue of SCN1A, Asn1788Lys, was identified as a de novo mutation in an individual with Dravet syndrome, another early-onset epileptic encephalopathy.[22] The following abbreviations are used: h, human; a, anole lizard; f, fish (*Fugu*); Dm, *Drosophila melanogaster*; para, fly voltage-gated sodium channel (encoded by *paralytic*); hSCN5A, human cardiac sodium channel; hSCN1A, human neuronal sodium channel; N, Asn; D, Asp; and K, Lys. Dots represent amino acid identity.

To identify potential *cis*-acting regulatory variants in the whole-genome sequence, we also evaluated 44,851 variants within the 5′ UTR or within 1 kb upstream of the transcription start site. Of these, 80 qualified as potential de novo variants in the proband. After applying the same filtering approach as above, we identified 23 putative de novo variants; however, none of these was validated as a true variant after Sanger sequencing. There were no de novo candidates (including within the 5′ UTR or 1 kb upstream of the transcription start site) on the proband's X chromosomes.

The single validated de novo variant was an A>G transition at nucleotide position 5302 (c.5302A>G [NCBI ss#477075913]) in the coding sequence of *SCN8A* (NM_014191.2, MIM 600702) and resulted in an asparagine (Asn) to aspartate (Asp) substitution at amino acid 1768 (p.Asn1768Asp). *SCN8A* is one of nine members of the gene family encoding the voltage-gated sodium-channel pore-forming alpha subunits.[19] The *SCN8A*-encoded channel, Nav1.6, is composed of four homologous domains, D1 to D4, each containing six transmembrane segments. The subcellular localization of Nav1.6 includes concentration at the axon initial segment and nodes of Ranvier, and it is widely expressed in the CNS, where it regulates firing patterns of excitatory and inhibitory neurons.[20] The mutated residue is located in the final transmembrane segment adjacent to the C-terminal cytoplasmic domain of the channel (Figure 1). Asn1768 is invariant in vertebrate and invertebrate sodium channels, as shown for representative examples in Figure 1. The substitution p.Asn1768Asp is predicted to be highly deleterious by Polyphen-2 analysis[21] (HumDiv score = 0.992; HumVar score = 0.990). Interestingly, an individual with another form of epileptic encephalopathy (Dravet syndrome) carries a de novo mutation in the corresponding residue of the related sodium-channel gene *SCN1A*,[22] although the actual functional consequence of this variant has not yet been assessed.

To evaluate the functional consequences of the de novo *SCN8A* mutation, we introduced the c.5302A>G nucleotide mutation into the tetrodotoxin (TTX)-resistant derivative of the Nav1.6 cDNA clone, $Nav1.6_R$.[23,24] To confirm the absence of additional mutations, we sequenced the entire 6 kb open reading frame prior to functional testing by transfection into the dorsal root ganglion (DRG) neuron-derived cell line ND7/23,[25] as previously described.[26] In the presence of 300 nM TTX, endogenous sodium currents are blocked, and currents derived from the transfected $Nav1.6_R$ clones can be studied in isolation.[26] Forty eight hours after transfection, cells with robust green fluorescence were selected for recording.

Representative families of traces of Na^+ currents from voltage-clamp recordings are shown in Figure 2A. The persistent currents that are detected 100 ms after the onset of step depolarization and normalized to peak transient current increased from an average of 1.8% for cells transfected with the wild-type (WT) channel to 13% for cells transfected with the mutant channel (Figure 2A insets and Table 1). Despite a 56% reduction in peak-current density for cells transfected with the mutant channel, the absolute values of the persistent current (61 ± 6 pA [n = 11] for WT; and 353 ± 51 pA [n = 11] for p.Asn1768Asp) and persistent-current density (2.02 ± 0.20 pA/pF [n = 11] for WT; and 10.51 ± 1.57 pA/pF [n = 11] for p.Asn1768Asp) were more than five times larger for the mutant channels. The voltage dependence of the persistent current is shown in Figure 2B, and it is greatest at +15 mV. The p.Asn1768Asp substitution also causes a 13 mV depolarizing shift in the voltage dependence of steady-state fast inactivation and increases the noninactivating component of the current (see arrow in Figure 2C). The development of closed-state inactivation is slower for the mutant channels (data for −60 mV shown in Figure 2D), and, as expected, p.Asn1768Asp channels produce a substantially enhanced (11 times larger) response to slow, ramp-like depolarizing stimuli (Figure 2E). All of these changes are known to increase neuronal excitability; it has been shown that persistent sodium currents contribute to the generation of paroxysmal depolarizing shifts (PDS), a cellular response predictive of recurrent seizures.[27] The mutation causes a small depolarizing shift of 4 mV in the voltage dependence of

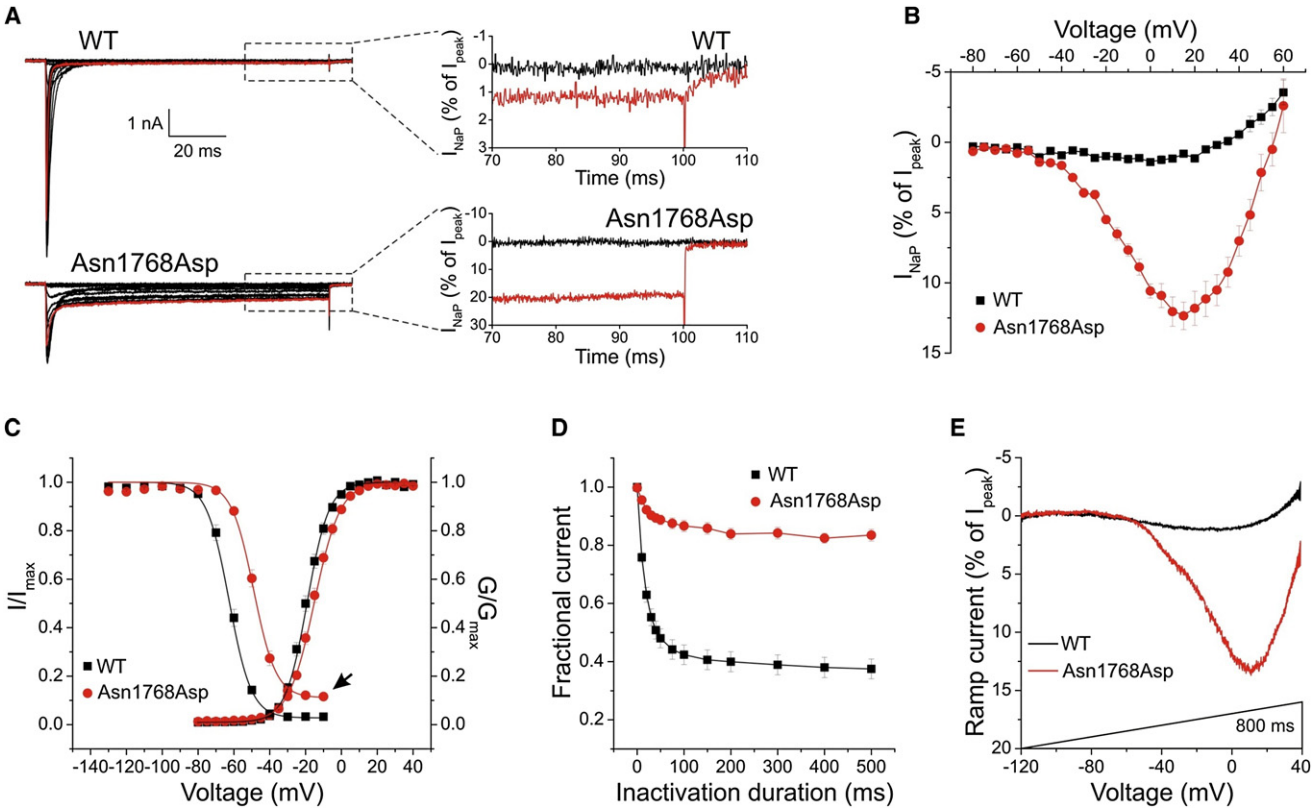

Figure 2. Effect of the De Novo SCN8A Substitution p.Asn1768Asp on Biophysical Properties of the Channel

(A) Representative inward currents recorded from ND7/23 cells transiently transfected with Nav1.6$_R$ WT or mutant channels. Cells were held at −120 mV, and a family of step depolarizations (−80 to +60 mV in 5 mV increments) were applied every 5 s. Insets show persistent inward currents (normalized by maximal transient peak currents) from WT and p.Asn1768Asp channels at the end of a 100 ms step depolarization to −80 mV (black) and +20 mV (red).

(B) Voltage dependence of persistent current. The amplitude of persistent current was measured as the mean value of currents 93–98 ms after the onset of depolarization and is presented as a percentage of the maximal transient peak current.

(C) Voltage dependence of channel activation and steady-state fast inactivation. Channel activation was analyzed as previously described.[26] Steady-state fast inactivation was assessed with a series of 100 ms step depolarizations (−130 to −10 mV in 10 mV increments) and was followed by a test pulse (−10 mV) so the remaining fraction of noninactivated channels could be measured. The p.Asn1768Asp channels do not completely inactivate, which is consistent with the large persistent current.

(D) Development of closed-state inactivation at −60 mV. Cells were held at −120 mV, and closed-state inactivation was assessed with a prepulse set to −60 mV with a duration varying from 0 to 500 ms, and remaining available channels were assessed with a test pulse set to 0 mV (20 ms).

(E) Mean ramp currents generated by WT (black) and p.Asn1768Asp (red) channels. The response to a slow ramp stimulus was evaluated with a ramp depolarization from −120 to +40 mV over 800 ms. The p.Asn1768Asp mutation increases the amplitude of the ramp current (normalized by transient peak current; p.Asn1768Asp [13.6 ± 1.9%, n = 5, $p < 0.05$] versus WT [1.2 ± 0.2%, n = 7]).

activation **(**Figure 2C**)** and shifts the voltage dependence of steady-state slow inactivation by −11.6 mV (not shown), which would reduce the proexcitatory effects.

The biophysical properties of p.Asn1768Asp channels are summarized in Table 1. In heterozygous neurons, mutant and WT alpha subunits would be coexpressed and act independently. The direction and magnitude of the proexcitatory effects of the p.Asn1768Asp substitution are consistent with a dominantly expressed phenotype of abnormal neuronal excitability. To test this prediction, we examined the firing patterns of cultured hippocampal neurons (dissociated from P10–P14 [postnatal days 10–14] Sprague Dawley rats) expressing transfected mutant and WT *Scn8a* cDNAs by using current-clamp recordings (Figures 3A–3C). Spontaneous firing was detected in 3/17 (18%) neurons transfected with the WT *Scn8a* cDNA and in a significantly higher percentage (10/17; 59%, $p < 0.05$) of neurons transfected with c.5302A>G (Figure 3B); these latter neurons also displayed PDS-like complexes (Figure 3Aii). In response to current injection, the frequency of action potentials was twice as high in cells expressing the mutant channels (Figure 3C). These observations demonstrate that expression of the mutant channel results in a phenotype of neuronal hyperexcitability, including increased spontaneous firing and PDS-like complexes.

Several factors support a causal role for the *SCN8A* c.5302A>G mutation in the phenotype observed in the proband: (1) *SCN8A* encodes a neuronal sodium channel that is highly abundant in the brain,[20,28] (2) the amino acid substitution produces a substantial increase in

Table 1. Biophysical Effects of the SCN8A p.Asn1768Asp Substitution

	I_{Na} Density (pA/pF)	$I_{persistent}$ (% of I_{peak})	Reversal Potential (mV)	Activation			Steady-State Fast Inactivation				Slow Inactivation			
				$V_{1/2,act}$	*k*	n	$V_{1/2,fast}$	*k*	A%	n	$V_{1/2,slow}$	*k*	A%	n
WT	130 ± 21 (20)	1.8 ± 0.3 (11)	69.0 ± 1.6	−19.5 ± 0.8	−6.16 ± 0.27	17	−62.1 ± 1.0	5.61 ± 0.11	2.85 ± 0.51	16	−41.7 ± 1.3	14.2 ± 0.5	3.84 ± 1.01	14
N1768D	57 ± 7[a] (24)	13.1 ± 0.9[a] (11)	71.0 ± 1.5	−15.3 ± 0.9[a]	−6.96 ± 0.25[a]	14	−48.7 ± 0.9[a]	5.77 ± 0.17	10.9 ± 0.86[a]	10	−53.3 ± 1.5[a]	6.5 ± 0.3[a]	2.15 ± 0.69	10

Whole-cell voltage-clamp recordings were performed with an Axopatch 200B amplifier (Molecular Devices, Sunnyvale, CA). The pipette solution contained (in mM) 140 CsF, 10 NaCl, 1 EGTA, 10 Dextrose, 10 HEPES (pH 7.3) (with CsOH), and osmolarity was adjusted to 315 mosmol/liter with sucrose. The extracellular bath solution contained (in mM) 140 NaCl, 3 KCl, 20 tetraethylammonium, 1 $MgCl_2$, 1 $CaCl_2$, 10 HEPES, 5 CsCl, 0.1 $CdCl_2$ (pH 7.3) (with NaOH); osmolarity was 325 mosmol/liter. 300 nM tetrodotoxin was added to the extracellular bath solution to block endogenous voltage-gated sodium currents in ND7/23.[26] All recordings were conducted at room temperature (~22°C). Currents were acquired with Clampex 9.2 5 min after establishing whole-cell configuration, sampled at 50 or 100 kHz, and filtered at 5 kHz. The following abbreviations are used: I_{Na}, voltage-gated sodium current; $I_{persistent}$, sodium current that is resistant to fast inactivation at the end of 100 ms step depolarization; I_{peak}, the maximal transient peak sodium current; $V_{1/2,act}$, the potential at which activation of sodium channels reaches half maximal; *k*, the slope factor; A%, the percentage of sodium channels that are resistant to fast inactivation or slow inactivation; n, number of cells.
[a]p value < 0.05 compared to WT.

persistent and ramp currents and results in neuronal hyperexcitability that includes increased spontaneous activity and PDS-like complexes, and (3) heterozygous mutations with similar properties in other closely related neuronal sodium channels cause epilepsy.[19] This result demonstrates the power of the WGS approach for unbiased discovery of pathogenic mutations in neurological disorders of unknown etiology. Causative variants in severe, early-onset neurological diseases are likely to be rare and distributed across many genes, some of which are not on candidate-gene lists.[29] This study presents the fifth member of the voltage-gated sodium-channel gene family to be implicated in seizure disorders; the other four are *SCN1A*, *SCN2A* (MIM 182390), *SCN3A* (MIM 182391), and *SCN9A* (MIM 603415).[19] In addition to *SCN1A* and the cardiac channel *SCN5A* (MIM 600163), *SCN8A* is the third sodium channel to be implicated in SUDEP, which accounts for deaths in up to 38% of people with epilepsies.[30] In this context, it is interesting that both *Scn1a* and *Scn8a* are expressed at a low level in cardiac myocytes,[31] and cardiac function is impaired in *Scn8a*-null mice.[32]

The in vivo physiological roles of Nav1.6 have been extensively studied in mice. The allele series of recessive *Scn8a* mutations includes missense, hypomorphic, and null alleles.[26,33–35] Motor deficits are prevalent because of the important role of Nav1.6 at nodes of Ranvier in motor neurons. Homozygotes for partial- and complete-loss-of-function alleles exhibit ataxic gait, tremor, dystonia, muscle atrophy, loss of hind-limb function, and juvenile lethality caused by loss of neurotransmitter release at the neuromuscular junction. The single previously reported *SCN8A* mutation is a premature stop codon identified in a proband with cerebellar ataxia; the mutation cosegregated with cognitive impairment but did not result in seizures.[36] Likewise, heterozygous $Scn8a^{+/-}$ mice exhibit an anxiety-like behavioral disorder but do not have spontaneous seizures.[37] Thus, haploinsufficiency of *SCN8A* does not cause epilepsy in humans or mice. However, spike-wave discharge patterns are seen in certain *Scn8a* heterozygotes,[38] and heterozygosity for an *Scn8a*-null allele can suppress seizures in an $Scn1a^{+/-}$ mouse model of Dravet syndrome,[39] demonstrating physiological interaction between these two sodium channels in determining neuronal excitability.

The mutation in the proband is a gain-of-function allele of *SCN8A* and causes a large increase in ramp and persistent currents and incomplete channel inactivation. Increased persistent current is a common characteristic of gain-of-function *SCN1A* mutations in individuals with generalized epilepsy with febrile seizures plus (GEFS+) and is characteristic of pathogenic mutations of *SCN2A* and *SCN3A*.[40–45] The Q54 mouse model expresses an *Scn2a* mutant channel with an elevated persistent current that causes a dominant seizure disorder.[46] Notably, transfection of hippocampal neurons with p.Asn1768Asp channels resulted in hyperexcitability that included increased spontaneous activity and PDS-like complexes. The effect of the proband's *SCN8A* mutation on the persistent current is considerably more severe than the reported examples in other channels, which strongly supports a causal role in the severe, dominant epileptic encephalopathy.

Mutations in *SCN1A* are the most common genetic cause of inherited and sporadic epilepsy, and >700 proband mutations, of which >80% are found in individuals with Dravet syndrome, have been reported thus far.[6,47,48] More than 90% of the *SCN1A* mutations in individuals with Dravet syndrome arose de novo and more than 50% are loss-of-function mutations, demonstrating that, unlike for *SCN8A*, haploinsufficiency for *SCN1A* results in seizures.[19,34] Our proband displays many features typically found in individuals with Dravet syndrome; one such feature is infancy-onset seizures that ultimately become refractory to therapeutic intervention and cause epileptic encephalopathy as a result of the regression of developmental abilities. However, consistent with a distinct genetic basis, there are also important differences: (1) Our proband did not manifest prolonged generalized convulsive or unilateral febrile and afebrile seizures in the first year of life; (2) rather than display distinct myoclonic and generalized

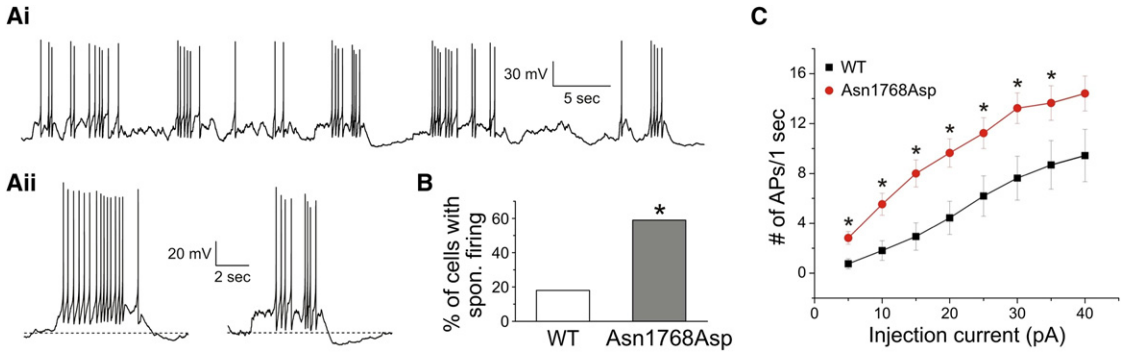

Figure 3. Effect of the De Novo SCN8A Substitution p.Asn1768Asp on Hippocampal Neuronal Excitability
(A) p.Asn1768Asp channels increase excitability of hippocampal neurons. (Ai) An example of spontaneous firing in a neuron transfected with p.Asn1768Asp channels. (Aii) Representative PDS-like complexes recorded from two hippocampal pyramidal neurons transfected with p.Asn1768Asp. The dashed lines indicate −80 mV.
(B) Percentage of neurons displaying spontaneous firing. The asterisk indicates $p < 0.05$.
(C) Number of action potentials (APs) evoked by a series of 1 s step depolarizating current injections (from 5 to 40 pA with a 5 pA increment). Neurons transfected with p.Asn1768Asp produce more APs than neurons transfected with WT. An asterisk indicates $p < 0.05$.

convulsive seizures as seen in typical Dravet syndrome, our proband had late-onset epileptic spasms characterized by repetitive clusters of jerks with the classical EEG pattern of spasms (i.e., high-amplitude delta wave followed by background suppression); and (3) a period of normal development was not seen in our proband. Delineating the clinical variability within this group and distinguishing the phenotypes of carriers of pathogenic mutations in *SCN8A* and *SCN1A* will require further characterization of individuals with *SCN8A* mutations.

We also evaluated the WGS data from our quartet for a model of inherited homozygous recessive disease. Variants with a frequency >1% in the 1,000 Genomes Project or in the CG public genomes were excluded as potential candidates. Seven genes fit a recessive inheritance pattern in the proband only (Table S2). Two of these (*NRP2* and *UNC13C*) were cases of compound heterozygosity that appeared functionally relevant on the basis of the Autworks database and biomedical literature. Both parents were heterozygous for nonsynonymous variants in *NRP2* (*neuropilin 2*, MIM 602070) and *UNC13C* (unc-13 homolog C [*C. elegans*]). The inherited variants were predicted to be deleterious by PolyPhen-2 analysis (HumDiv > 0.993) and were extremely rare; they had frequencies <1% in the National Heart, Lung, and Blood Institute (NHLBI) Exome Sequencing Project (see Web Resources). The maternally inherited *NRP2* allele, also transmitted to the brother, is c.1000C>T (p.Arg334Cys) (rs14144673), whereas the paternally inherited allele is c.1282C>T (p.Arg428Trp) (rs139711818). The maternally inherited *UNC13C* allele is c.912C>G (p.Asp304Glu) (rs149448818), and the paternally inherited allele is c.6587T>C (p.Val2196Ala) (rs146433220).

NRP2 is a transmembrane receptor for class 3 semaphorins, secreted proteins that are essential for guiding axon pathfinding and sorting during central- and peripheral-nervous-system development.[49] *NRP2* polymorphisms have been associated with autism,[50] and *NRP2* is a candidate gene for juvenile myoclonic epilepsy.[51] *Nrp2*-deficient mice display increased neuronal excitability and susceptibility to chemically induced seizures.[52] Loss-of-function *Nrp2* mutations in homozygous mice cause defects of axon-tract formation, such as the misrouting, disorganization, or loss of fiber bundles.[49] Moreover, loss of Nrp2 causes increased cortical and hippocampal dendritic-spine numbers[53] and decreased numbers of hippocampal interneurons and GABAergic synapses.[52] The *UNC13* gene family encodes highly conserved proteins, most of which are expressed in neurons, where they serve a crucial function in synaptic-vesicle fusion for neurotransmitter release.[54,55] Disrupting the function of any single *Unc13* gene can impair neuronal function, including synaptic plasticity[56] and motor learning,[57] in mouse mutants without disrupting neuronal morphology.

It has often been suggested that the inheritance of modifier loci contributes to the wide phenotypic variability of individuals with *SCN1A* mutations.[19] With WGS data, it is now possible to predict the identity of specific candidate modifier variants in individuals. In the present case, *NRP2* variants could plausibly enhance seizures through neuronal hyperexcitability and the loss of inhibitory synapses, whereas *UNC13C* variants could reduce seizure activity by inhibiting synaptic-vesicle release and thereby increasing the threshold for synaptic transmission. Testing the role of genetic interactions in modifying the phenotypic expression of *SCN8A* gain-of-function mutations will require new animal models.

In summary, by performing high-coverage WGS on a family quartet, we have identified a de novo *SCN8A* mutation that can account for the epileptic encephalopathy that eventually resulted in SUDEP in the proband. Recent whole-genome and whole-exome approaches have been remarkably successful in identifying amino-acid-altering de novo mutations in individuals with severe neurological disorders. However, in most cases to date, direct support for causality has been lacking, and knowledge of the gene or

protein function has allowed only predictions about the consequences of a particular mutation. We have confirmed the pathogenicity of our candidate *SCN8A* c.5302A>G mutation through the biophysical characterization of the channel and electrophysiological analysis in primary neurons. Given the likely importance of rare variants with large effects in disease etiology,[5,58] such follow-up functional analysis will be vital as an increasing number of de novo or extremely rare variants are discovered through WGS of probands and their families.

Supplemental Data

Supplemental Data include two tables and can be found with this article online at http://www.cell.com/AJHG.

Acknowledgments

Support for this work was provided by the National Institutes of Health to K.R.V. (R01_HG005226), M.H.M. (R01_NS34509), J.E.O. (T32_GM007544), and E.E.E. (HD065285). S.G.W. and S.D.H. are funded by grants from the Veterans Administration Medical Research Service and Rehabilitation Research Service. This work was also supported by the Simons Foundation Autism Research Initiative (E.E.E.). E.E.E. is an investigator of the Howard Hughes Medical Institute. L.L.R. is funded by Autism Speaks and the Arizona Center for Biology of Complex Diseases. We thank Tanya Karafet, Daniel Wolf, and Kimiko Della Croce for the de novo variant validation by PCR and sequencing.

Received: November 28, 2011
Revised: December 20, 2011
Accepted: January 9, 2012
Published online: February 23, 2012

Web Resources

The URLs for data presented herein are as follows:

1000 Genomes May 2011 Data Release, http://www.1000genomes.org/node/506/
ANNOVAR, http://www.openbioinformatics.org/annovar/
Autworks, http://autworks.hms.harvard.edu/
Complete Genomics Incorporated Public Genomes, ftp://ftp2.completegenomics.com
Database of Genomic Variants (DGV), http://projects.tcag.ca/variation/
NHLBI Exome Sequencing Project, http://evs.gs.washington.edu/EVS/
Online Mendelian Inheritance in Man (OMIM), http://www.omim.org
PolyPhen2, http://genetics.bwh.harvard.edu/pph2/
SCN1A Variant database, http://www.molgen.ua.ac.be/SCN1AMutations/
UCSC Known Genes database, http://genome.ucsc.edu/

References

1. Bamshad, M.J., Ng, S.B., Bigham, A.W., Tabor, H.K., Emond, M.J., Nickerson, D.A., and Shendure, J. (2011). Exome sequencing as a tool for Mendelian disease gene discovery. Nat. Rev. Genet. *12*, 745–755.
2. Mitchell, K.J. (2011). The genetics of neurodevelopmental disease. Curr. Opin. Neurobiol. *21*, 197–203.
3. Morrow, E.M. (2010). Genomic copy number variation in disorders of cognitive development. J. Am. Acad. Child Adolesc. Psychiatry *49*, 1091–1104.
4. Girirajan, S., and Eichler, E.E. (2010). Phenotypic variability and genetic susceptibility to genomic disorders. Hum. Mol. Genet. *19* (R2), R176–R187.
5. Gorlov, I.P., Gorlova, O.Y., Frazier, M.L., Spitz, M.R., and Amos, C.I. (2011). Evolutionary evidence of the effect of rare variants on disease etiology. Clin. Genet. *79*, 199–206.
6. Marini, C., Scheffer, I.E., Nabbout, R., Suls, A., De Jonghe, P., Zara, F., and Guerrini, R. (2011). The genetics of Dravet syndrome. Epilepsia *52* (*Suppl 2*), 24–29.
7. Pavone, P., Spalice, A., Polizzi, A., Parisi, P., and Ruggieri, M. (2011). Ohtahara syndrome with emphasis on recent genetic discovery. Brain Dev., in press.
8. Conrad, D.F., Keebler, J.E.M., DePristo, M.A., Lindsay, S.J., Zhang, Y., Casals, F., Idaghdour, Y., Hartl, C.L., Torroja, C., Garimella, K.V., et al; 1000 Genomes Project. (2011). Variation in genome-wide mutation rates within and between human families. Nat. Genet. *43*, 712–714.
9. Roach, J.C., Glusman, G., Smit, A.F.A., Huff, C.D., Hubley, R., Shannon, P.T., Rowen, L., Pant, K.P., Goodman, N., Bamshad, M., et al. (2010). Analysis of genetic inheritance in a family quartet by whole-genome sequencing. Science *328*, 636–639.
10. Sepp, K.J., Hong, P., Lizarraga, S.B., Liu, J.S., Mejia, L.A., Walsh, C.A., and Perrimon, N. (2008). Identification of neural outgrowth genes using genome-wide RNAi. PLoS Genet. *4*, e1000111.
11. Lynch, M. (2010). Rate, molecular spectrum, and consequences of human mutation. Proc. Natl. Acad. Sci. USA *107*, 961–968.
12. Vissers, L.E.L.M., de Ligt, J., Gilissen, C., Janssen, I., Steehouwer, M., de Vries, P., van Lier, B., Arts, P., Wieskamp, N., del Rosario, M., et al. (2010). A de novo paradigm for mental retardation. Nat. Genet. *42*, 1109–1112.
13. O'Roak, B.J., Deriziotis, P., Lee, C., Vives, L., Schwartz, J.J., Girirajan, S., Karakoc, E., Mackenzie, A.P., Ng, S.B., Baker, C., et al. (2011). Exome sequencing in sporadic autism spectrum disorders identifies severe de novo mutations. Nat. Genet. *43*, 585–589.
14. Girard, S.L., Gauthier, J., Noreau, A., Xiong, L., Zhou, S., Jouan, L., Dionne-Laporte, A., Spiegelman, D., Henrion, E., Diallo, O., et al. (2011). Increased exonic de novo mutation rate in individuals with schizophrenia. Nat. Genet. *43*, 860–863.
15. Dewey, F.E., Chen, R., Cordero, S.P., Ormond, K.E., Caleshu, C., Karczewski, K.J., Whirl-Carrillo, M., Wheeler, M.T., Dudley, J.T., Byrnes, J.K., et al. (2011). Phased whole-genome genetic risk in a family quartet using a major allele reference sequence. PLoS Genet. *7*, e1002280.
16. Cooper, G.M., Coe, B.P., Girirajan, S., Rosenfeld, J.A., Vu, T.H., Baker, C., Williams, C., Stalker, H., Hamid, R., Hannig, V., et al. (2011). A copy number variation morbidity map of developmental delay. Nat. Genet. *43*, 838–846.
17. Drmanac, R., Sparks, A.B., Callow, M.J., Halpern, A.L., Burns, N.L., Kermani, B.G., Carnevali, P., Nazarenko, I., Nilsen, G.B., Yeung, G., et al. (2010). Human genome sequencing using unchained base reads on self-assembling DNA nanoarrays. Science *327*, 78–81.

18. Wang, K., Li, M., and Hakonarson, H. (2010). ANNOVAR: Functional annotation of genetic variants from high-throughput sequencing data. Nucleic Acids Res. *38*, e164.
19. Meisler, M.H., O'Brien, J.E., and Sharkey, L.M. (2010). Sodium channel gene family: Epilepsy mutations, gene interactions and modifier effects. J. Physiol. *588*, 1841–1848.
20. O'Brien, J.E., Drews, V.L., Jones, J.M., Dugas, J.C., Barres, B.A., and Meisler, M.H. (2011). Rbfox proteins regulate alternative splicing of neuronal sodium channel SCN8A. Mol Cell Neurosci. *49*, 120–126.
21. Adzhubei, I.A., Schmidt, S., Peshkin, L., Ramensky, V.E., Gerasimova, A., Bork, P., Kondrashov, A.S., and Sunyaev, S.R. (2010). A method and server for predicting damaging missense mutations. Nat. Methods *7*, 248–249.
22. Depienne, C., Trouillard, O., Saint-Martin, C., Gourfinkel-An, I., Bouteiller, D., Carpentier, W., Keren, B., Abert, B., Gautier, A., Baulac, S., et al. (2009). Spectrum of SCN1A gene mutations associated with Dravet syndrome: analysis of 333 patients. J. Med. Genet. *46*, 183–191.
23. Herzog, R.I., Cummins, T.R., Ghassemi, F., Dib-Hajj, S.D., and Waxman, S.G. (2003). Distinct repriming and closed-state inactivation kinetics of Nav1.6 and Nav1.7 sodium channels in mouse spinal sensory neurons. J. Physiol. *551*, 741–750.
24. Dib-Hajj, S.D., Choi, J.S., Macala, L.J., Tyrrell, L., Black, J.A., Cummins, T.R., and Waxman, S.G. (2009). Transfection of rat or mouse neurons by biolistics or electroporation. Nat. Protoc. *4*, 1118–1126.
25. Wood, J.N., Bevan, S.J., Coote, P.R., Dunn, P.M., Harmar, A., Hogan, P., Latchman, D.S., Morrison, C., Rougon, G., Theveniau, M., et al. (1990). Novel cell lines display properties of nociceptive sensory neurons. Proc. Biol. Sci. *241*, 187–194.
26. Sharkey, L.M., Cheng, X., Drews, V., Buchner, D.A., Jones, J.M., Justice, M.J., Waxman, S.G., Dib-Hajj, S.D., and Meisler, M.H. (2009). The ataxia3 mutation in the N-terminal cytoplasmic domain of sodium channel Na(v)1.6 disrupts intracellular trafficking. J. Neurosci. *29*, 2733–2741.
27. Chen, S., Su, H., Yue, C., Remy, S., Royeck, M., Sochivko, D., Opitz, T., Beck, H., and Yaari, Y. (2011). An increase in persistent sodium current contributes to intrinsic neuronal bursting after status epilepticus. J. Neurophysiol. *105*, 117–129.
28. Schaller, K.L., and Caldwell, J.H. (2000). Developmental and regional expression of sodium channel isoform NaCh6 in the rat central nervous system. J. Comp. Neurol. *420*, 84–97.
29. Lu, Y., and Wang, X. (2009). Genes associated with idiopathic epilepsies: A current overview. Neurol. Res. *31*, 135–143.
30. Devinsky, O. (2011). Sudden, unexpected death in epilepsy. N. Engl. J. Med. *365*, 1801–1811.
31. Maier, S.K., Westenbroek, R.E., McCormick, K.A., Curtis, R., Scheuer, T., and Catterall, W.A. (2004). Distinct subcellular localization of different sodium channel alpha and beta subunits in single ventricular myocytes from mouse heart. Circulation *109*, 1421–1427.
32. Noujaim, S.F., Kaur, K., Milstein, M., Jones, J.M., Furspan, P., Jiang, D., Auerbach, D.S., Herron, T., Meisler, M.H., and Jalife, J. (2012). A null mutation of the neuronal sodium channel NaV1.6 disrupts action potential propagation and excitation-contraction coupling in the mouse heart. FASEB J. *26*, 63–72. Published online September 24, 2011.
33. Burgess, D.L., Kohrman, D.C., Galt, J., Plummer, N.W., Jones, J.M., Spear, B., and Meisler, M.H. (1995). Mutation of a new sodium channel gene, Scn8a, in the mouse mutant 'motor endplate disease'. Nat. Genet. *10*, 461–465.
34. Meisler, M.H., and Kearney, J.A. (2005). Sodium channel mutations in epilepsy and other neurological disorders. J. Clin. Invest. *115*, 2010–2017.
35. Meisler, M.H., Plummer, N.W., Burgess, D.L., Buchner, D.A., and Sprunger, L.K. (2004). Allelic mutations of the sodium channel SCN8A reveal multiple cellular and physiological functions. Genetica *122*, 37–45.
36. Trudeau, M.M., Dalton, J.C., Day, J.W., Ranum, L.P., and Meisler, M.H. (2006). Heterozygosity for a protein truncation mutation of sodium channel SCN8A in a patient with cerebellar atrophy, ataxia, and mental retardation. J. Med. Genet. *43*, 527–530.
37. McKinney, B.C., Chow, C.Y., Meisler, M.H., and Murphy, G.G. (2008). Exaggerated emotional behavior in mice heterozygous null for the sodium channel Scn8a (Nav1.6). Genes Brain Behav. *7*, 629–638.
38. Papale, L.A., Beyer, B., Jones, J.M., Sharkey, L.M., Tufik, S., Epstein, M., Letts, V.A., Meisler, M.H., Frankel, W.N., and Escayg, A. (2009). Heterozygous mutations of the voltage-gated sodium channel SCN8A are associated with spike-wave discharges and absence epilepsy in mice. Hum. Mol. Genet. *18*, 1633–1641.
39. Martin, M.S., Tang, B., Papale, L.A., Yu, F.H., Catterall, W.A., and Escayg, A. (2007). The voltage-gated sodium channel Scn8a is a genetic modifier of severe myoclonic epilepsy of infancy. Hum. Mol. Genet. *16*, 2892–2899.
40. Estacion, M., Gasser, A., Dib-Hajj, S.D., and Waxman, S.G. (2010). A sodium channel mutation linked to epilepsy increases ramp and persistent current of Nav1.3 and induces hyperexcitability in hippocampal neurons. Exp. Neurol. *224*, 362–368.
41. Holland, K.D., Kearney, J.A., Glauser, T.A., Buck, G., Keddache, M., Blankston, J.R., Glaaser, I.W., Kass, R.S., and Meisler, M.H. (2008). Mutation of sodium channel SCN3A in a patient with cryptogenic pediatric partial epilepsy. Neurosci. Lett. *433*, 65–70.
42. Liao, Y., Anttonen, A.K., Liukkonen, E., Gaily, E., Maljevic, S., Schubert, S., Bellan-Koch, A., Petrou, S., Ahonen, V.E., Lerche, H., and Lehesjoki, A.E. (2010). SCN2A mutation associated with neonatal epilepsy, late-onset episodic ataxia, myoclonus, and pain. Neurology *75*, 1454–1458.
43. Spampanato, J., Escayg, A., Meisler, M.H., and Goldin, A.L. (2001). Functional effects of two voltage-gated sodium channel mutations that cause generalized epilepsy with febrile seizures plus type 2. J. Neurosci. *21*, 7481–7490.
44. Vanoye, C.G., Lossin, C., Rhodes, T.H., and George, A.L., Jr. (2006). Single-channel properties of human NaV1.1 and mechanism of channel dysfunction in SCN1A-associated epilepsy. J. Gen. Physiol. *127*, 1–14.
45. Volkers, L., Kahlig, K.M., Verbeek, N.E., Das, J.H., van Kempen, M.J., Stroink, H., Augustijn, P., van Nieuwenhuizen, O., Lindhout, D., George, A.L., Jr., et al. (2011). Nav 1.1 dysfunction in genetic epilepsy with febrile seizures-plus or Dravet syndrome. Eur. J. Neurosci. *34*, 1268–1275.
46. Kearney, J.A., Plummer, N.W., Smith, M.R., Kapur, J., Cummins, T.R., Waxman, S.G., Goldin, A.L., and Meisler, M.H. (2001). A gain-of-function mutation in the sodium channel gene Scn2a results in seizures and behavioral abnormalities. Neuroscience *102*, 307–317.
47. Catterall, W.A., Dib-Hajj, S., Meisler, M.H., and Pietrobon, D. (2008). Inherited neuronal ion channelopathies: new windows on complex neurological diseases. J. Neurosci. *28*, 11768–11777.

48. Poduri, A., and Lowenstein, D. (2011). Epilepsy genetics—past, present, and future. Curr. Opin. Genet. Dev. *21*, 325–332.
49. Pellet-Many, C., Frankel, P., Jia, H., and Zachary, I. (2008). Neuropilins: Structure, function and role in disease. Biochem. J. *411*, 211–226.
50. Wu, S., Yue, W., Jia, M., Ruan, Y., Lu, T., Gong, X., Shuang, M., Liu, J., Yang, X., and Zhang, D. (2007). Association of the neuropilin-2 (NRP2) gene polymorphisms with autism in Chinese Han population. Am. J. Med. Genet. B. Neuropsychiatr. Genet. *144B*, 492–495.
51. Ratnapriya, R., Vijai, J., Kadandale, J.S., Iyer, R.S., Radhakrishnan, K., and Anand, A. (2010). A locus for juvenile myoclonic epilepsy maps to 2q33-q36. Hum. Genet. *128*, 123–130.
52. Gant, J.C., Thibault, O., Blalock, E.M., Yang, J., Bachstetter, A., Kotick, J., Schauwecker, P.E., Hauser, K.F., Smith, G.M., Mervis, R., et al. (2009). Decreased number of interneurons and increased seizures in neuropilin 2 deficient mice: Implications for autism and epilepsy. Epilepsia *50*, 629–645.
53. Tran, T.S., Rubio, M.E., Clem, R.L., Johnson, D., Case, L., Tessier-Lavigne, M., Huganir, R.L., Ginty, D.D., and Kolodkin, A.L. (2009). Secreted semaphorins control spine distribution and morphogenesis in the postnatal CNS. Nature *462*, 1065–1069.
54. Basu, J., Betz, A., Brose, N., and Rosenmund, C. (2007). Munc13-1 C1 domain activation lowers the energy barrier for synaptic vesicle fusion. J. Neurosci. *27*, 1200–1210.
55. Brose, N., Rosenmund, C., and Rettig, J. (2000). Regulation of transmitter release by Unc-13 and its homologues. Curr. Opin. Neurobiol. *10*, 303–311.
56. Rosenmund, C., Sigler, A., Augustin, I., Reim, K., Brose, N., and Rhee, J.S. (2002). Differential control of vesicle priming and short-term plasticity by Munc13 isoforms. Neuron *33*, 411–424.
57. Augustin, I., Korte, S., Rickmann, M., Kretzschmar, H.A., Südhof, T.C., Herms, J.W., and Brose, N. (2001). The cerebellum-specific Munc13 isoform Munc13-3 regulates cerebellar synaptic transmission and motor learning in mice. J. Neurosci. *21*, 10–17.
58. Robinson, P.N., Krawitz, P., and Mundlos, S. (2011). Strategies for exome and genome sequence data analysis in disease-gene discovery projects. Clin. Genet. *80*, 127–132.